Is Solar Hydrogen a Viable Solution for Energetically Self-Sustainable Off-Grid Buildings?

Stefania Perrella – University of Calabria, Italy – stefania.perrella@unical.it
Roberto Bruno – University of Calabria, Italy – roberto.bruno@unical.it
Piero Bevilacqua – University of Calabria, Italy – piero.bevilacqua@unical.it
Daniela Cirone – University of Calabria, Italy – daniela.cirone@unical.it

Abstract

A micro-cogeneration solution based on an alkaline fuel cell, supplied by solar hydrogen to satisfy electric and thermal energy demands in an off-grid building, is investigated. Hydrogen is produced by using PV surpluses through an alkaline electrolyzer and stored in a pressurized gas tank. Regarding a reference building with a gross footprint of 100 m² affected by severe winter climate conditions and heated by a radiant floor supplied by an air-water heat pump, TRNSYS simulations showed that 14.4 kW_P of PV power and 5 m³ of hydrogen tank volume ensure the building energy self-sustainability. Indoor comfort conditions are achieved by observing air temperatures always in the range of 19–21 °C during winter. The thermal power recovered from the fuel cell reduced DHW demand noticeably. Results show that hydrogen acts as an inter-seasonal storage with summer overproductions needed for the fuel-cell winter operation. An economic analysis confirms that the system is profitable when compared with electric storage made of batteries periodically replaced.

1. Introduction

The building energy requirements in the EU are responsible for more than 36% of greenhouse emissions (UN Environmental Program, 2024). Energy requalification of the existing stock is effortlessly achievable in grid-connected buildings by installing heat pumps driven by PV generators with suitable emitters, in which proper management of the electric surpluses is attainable even without energy storage systems (Perrella et al., 2024). Evident difficulties remain in off-grid buildings that, conversely, require the installation of storage systems to meet both electric and thermal requirements (Hakimi & Hasankhani, 2020) with energy's self-sustainability attained by reserves of fossil primary sources, preferred for the easy refuelling and the favourable costs. To limit the worsening of the environmental footprint, micro-cogeneration systems integrated with renewable sources to provide heat and electricity simultaneously could be used (Kallio & Siroux, 2022). However, the intermittence of solar irradiance makes the match between energy production and consumption difficult. A feasible solution is given by PV/T generators interacting with water tanks and batteries to manage thermal and electrical surpluses (Gugul, 2023). Nevertheless, accurate management of thermal energy is required to avoid a worsening of the PV cells' performance due to thermal drift effects (Bevilacqua et al., 2020). An alternative solution suitable in off-grid buildings is represented by alkaline fuel cells (AFC), which convert the chemical energy of hydrogen into electric and thermal energy, after that an electrolysis process driven by PV generators makes available the pressurized gas in proper tanks. AFCs are safe with a lifespan of over 20 years if supplied by pure hydrogen. In this paper, the performances of a cogenerative AFC, installed in a reference off-grid building, are explored. AFC is supplied by solar hydrogen produced by managing PV surpluses that drive an alkaline electrolyzer, producing pressurized hydrogen and oxygen. Electric energy is absorbed for base loads (lighting and appliances) and to supply an electric air-water heat pump that heats the building through a radiant floor. AFC thermal power is recovered in a water tank, equipped with an integrative electric resistance, for the supply of DHW at

Part of
Pernigotto, G., Ballarini, I., Patuzzi, F., Prada, A., Corrado, V., & Gasparella, A. (Eds.). 2025. Building simulation applications BSA 2024. bu,press.
https://doi.org/10.13124/9788860462022

least 45 °C. The components interaction (PV panels, electrolyzer, AFC, hydrogen tank, water tank, air-water heat pump, building), was simulated in TRNSYS (VV.AA., 2018) under a severe winter climate. Indeed, AFC, electrolyser and hydrogen storage have been largely studied by TRNSYS in the past, as reported in Wei et al. (2022) which evaluated solar panels and wind turbines to drive electrolysis in Canada. In Dezhdar et al. (2023) a hybrid storage system including batteries and hydrogen tanks was studied through TRNSYS simulations. Zeng et al. (2023) used TRNSYS to design an energy system based on AFC and hydrogen storage in China. Saleem et al. (2020) considered different configurations of solar-hydrogen generation systems in diverse climates. Many investigations were validated by experimental data, therefore TRNSYS is a reliable tool for simulating solar hydrogen as a "sui-generis" storage system to manage energy surpluses in grid-connected buildings. Conversely, in this paper, TRNSYS is used for sizing the components that ensure thermal and electric self-sustainability in an isolated building. An economic analysis compared this solution with an alternative system made of conventional batteries to verify its profitability.

2. Methodology

2.1 Off-Grid Building Features

The (real) isolated single-storey building (plant gross area 100 m², net inter-floor height of 2.80 m) with an unheated attic was modelled geometrically by SketchUp® and thermodynamically by TRNBUILD. The proposed plant could be hosted in a disused barn of 60 m² adjacent to the building. A sketch of two building prospects is shown in Fig. 1.

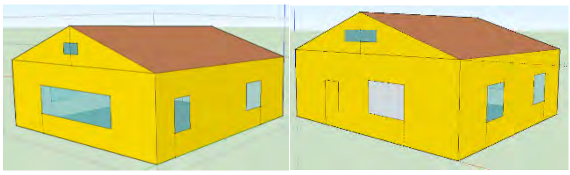

Fig. 1 – NW and SE prospects of the reference off-grid building

The building was simulated as a single thermal zone heated by a radiant floor. The roof pitches (53 m² each) are oriented East and West tilted at 15° to host PV arrays. The Window-to-Wall ratio is 9%, 12%, 10% and 25% respectively for South, East, West and North. Vertical opaque walls have a U-value of 0.248 W/(m²K), the ground floor has an equivalent U-value of 0.284 W/(m²K) and the ceiling deck (unheated attic as upper boundary condition) has 0.402 W/(m²K). The window U-value (wooden frame hosting a 4/15/4 system with low-ε panes) is 1.40 W/(m²K) with a normal solar factor of 0.589. Fig. 2 shows indoor air temperature and heating load profiles for an indoor set-point of 20 °C. The maximum heating load is 5.4 kW, the more frequent value is 3.8 kW and the heating requirement is 167 kWh/m². No cooling power is required in summer to set 26 °C.

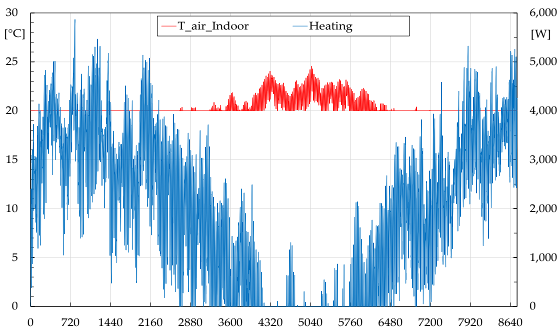

Fig. 2 – Hourly profiles of indoor air temperature and heating loads for an indoor set-point of 20 °C in the considered climatic zone

The intended use is a farmhouse with yearly average daily demands for DHW and electricity depicted in Fig. 3, based on a typical occupation pattern (Pflugradt, 2024). The electric profile refers exclusively to the base load, mainly concentrated in the central and evening hours, whereas DHW demand is distributed among early morning, midday and evening. The 80 m² of active radiant floor was simulated as an active layer, made of serpentine polymeric pipes (k=0.35 W/(m·K)) drowned in 5 cm of lightweight concrete, over a floor deck of 20 cm to use as thermal storage, externally insulated by 10 cm of EPS (k=0.035 W/(mK)). The pipe's pitch is 5 cm with an internal diameter of 10 mm, supplied by a constant water flow rate of 0.33 kg/s and variable inlet temperature. The heat pump is activated when a zone thermostat measures indoor air temperature under 19 °C (dead band 2 °C).

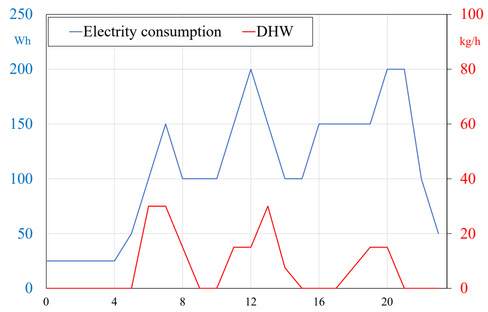

Fig. 3 – Yearly average daily profiles concerning electric base consumptions and DHW

2.2 Climatic Data

The building site has an altitude of 1440 m above sea level with 2897 HDD (Heating Degree Day), classified as Csb following the Koppen rating. Climatic data are provided by a TMY file: Fig. 4a) shows the trend of the outdoor air temperature whereas Fig. 4b) the horizontal solar irradiance.

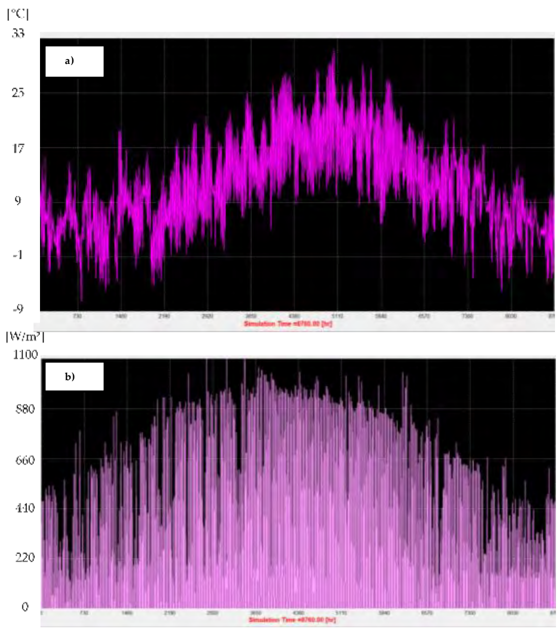

Fig. 4 – Hourly outdoor air temperature (a) and solar irradiation on the horizontal plane (b) for the considered site

2.3 Main Plant Components

2.3.1 Air-Water Heat Pump

The heat pump (HP) performances are determined as a function of the outdoor air and the supplied water temperatures. The device is equipped with an inverter avoiding the COP penalization in part-load mode. Following the heating loads depicted in Fig. 2, the heat pump rated heating capacity (outdoor air temperature at 7 °C and supplied hot water at 45 °C) is 6 kW with a corresponding COP of 3.46. The real COP, determined by associating a proper file describing the performance curves provided by the manufacturer (see Fig. 5), allows for the calculation of the real share of absorbed electricity.

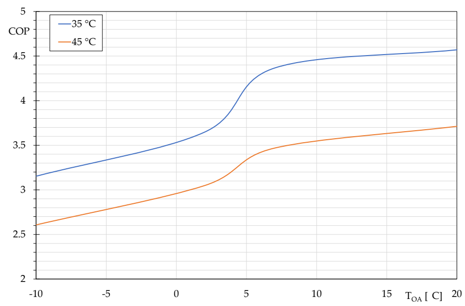

Fig. 5 – Heat pump COP as a function of the outdoor air temperature (T_{OA}) for two values of the supplied hot water

2.3.2 PV generator

Electric energy is provided directly by PV panels made of mono-crystalline cells installed coplanar with the roof pitches. The caption surface was set as a parameter for the system design. The panel peak power is 450 W with a rated efficiency of 20.6%. Temperature coefficients for current and voltage are respectively +0.044 %/°C and -0.272 %/°C needed to consider the thermal drift effect and the efficiency decrement. The projection of the solar radiation on the caption surface was carried out by the Reindl model. Electric surpluses drive an electrolyzer for hydrogen production and the maximum installable power is 21.6 kW_P.

2.3.3 Electrolyzer

The electrolyzer produces water electrolysis and gas compression to facilitate storage. It is constituted by a single stack with 21 cells in series and an electrode surface area of 0.25 m^2, operating at a constant pressure of 7 bar. The electrolyzer is designed to operate in a variable power mode through a specific conditioning power unit: when it is ON, the setpoint power is set to the maximum between the excess of power and an idling power that, for the considered device, was set to 500 W. Conversely, the electrolyzer is set OFF so that the PV surplus lower than 500 W is dissipated in the integrative electric resistance of the water tank's (800 litres). The electrolyzer control depends also on the state of charge (SoC) of the pressurized hydrogen storage: if it exceeds 0.95, the electrolyzer is OFF and the total surplus is used again for DHW production, to restart when the SoC goes down to 0.7 to confer control stability.

2.3.4 Hydrogen pressurized tank

This tank is charged by the electrolyzer whereas it is discharged to supply the fuel cell. The transient mass balance must be verified in every timestep, considering that the gas tank is subjected to a constant hydrogen consumption, depending on the Fuel Cell size, but variable hydrogen supply due to the magnitude of the PV surplus. A halved tank manages the oxygen storage. The tank volume is another parameter varied for the system design.

2.3.5 Alkaline Fuel Cell (AFC)

The fuel cell is made of 2 stacks in parallel equipped with 32 modules in series each, to obtain 220 V as output voltage (operating voltage of 7.374 V per module) with an electrode area of 100 cm^2. An empirical relationship describes the current-voltage characteristic at normal operating temperature. The generated heat is calculated simplistically without detailed dynamic thermal models but following the approach proposed by (Brown et al., 2001) setting a stack operating temperature of 70 °C when crossed by a current of 8.1 A. An internal heat exchanger recovers thermal power for the DHW tank. The AFC is activated also in diurnal hours when the sum of base loads, HP absorbed power and the water tank's resistance is greater than PV output.

2.4 Mini-Grid Management

The flow chart in Fig. 6 shows how a mini-grid installed in the off-grid building verifies the electric fluxes for design purposes (BL=Base Load, HP=absorbed by heat pump, EL=Electrolyzer, PVP= PV power, PVS=PV surpluses, ER= surplus for water tank's electric resistance, DHW= electric resistance activated with temperature below 45 °C). The correct component sizes are verified if, in every simulation timestep, the produced power is greater than the required electric load:

$$AFC+PVP \geq BL + HP + DHW \quad \text{Eq. 1}$$

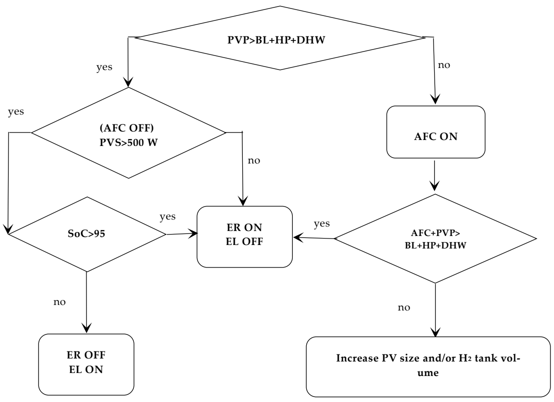

Fig. 6 – Electric fluxes management in the reference off-grid building carried out by an internal micro-grid

The non-absorbed power, detected when Eq. 1 provides positive results, is converted into thermal energy by the heat pump, stored in the building through the radiant floor (until the indoor air temperature is 21 °C) and in the water tank for DHW whose temperature can exceed 45 °C.

3. Results

Simulations started from 1^{st} January until 31^{st} December with a timestep of 1 minute. The following results are obtained starting with hydrogen storage full at 40 % (hypothesizing the accumulation of hydrogen overproduction in the previous summer). A parametric study has shown that the minimal plant configuration that ensures the verification of Eq. 1 in every timestep requires 14.4 kW_P of PV peak power (16 modules in series arranged in two arrays) and 5 m^3 of hydrogen storage volume (V). Fig. 7 depicts, for the coldest week (last week in January), the trends of the PV and AFC electric powers, and indoor air and operative temperatures. In contrast to the variable PV output, it is worth noting the constant (1,865 W) and misaligned power production from AFC. Simultaneous production was detected with scarce solar irradiance highlighted by the curves' overlap. In diurnal hours, AFC is not operating on sunny days due to the significant PV power production (over 9,000 W). Thermal energy for heating is managed adequately by detecting indoor air temperature that never falls under 19 °C, whereas overheating situations are avoided.

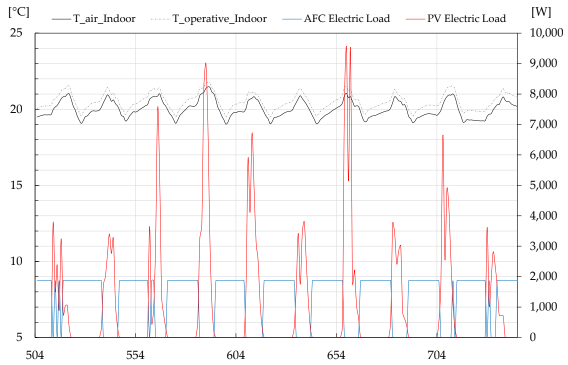

Fig. 7 – Temperature and power profiles for a plant configuration equipped with PV=14.4 kW_p and V=5m³ in January

Tab. 1 shows that the recovered thermal power from AFC ($\%E_{th,saved}$), of about 300 W, determines energy saving percentage varying between 70%-80% of the DHW demand (19 kWh/m^2). The PV surplus (PVS) managed by the electrolyzer and the water tank on an annual basis is over 18,000 kWh. Large shares are available in summer due to the limited heat pump operation. Fig. 8 shows that the main electric consumption source is represented by the heat pump in winter and the intermediate months, with consumptions that decrease with the outdoor air temperature growth. The water tank's electric resistance (1.2 kW) absorbs limited electricity, by benefiting from the thermal power recovered from the AFC. Tab. 1 shows that AFC (%AFC) intervenes mainly during the coldest months to compensate for the lower PV output. Annually 76.6% of power is provided by the PV generator (%PV). The hydrogen balance (H_2 Bal.) is negative in winter (absorption greater than production), however, larger productions in the other months prevent the pressurized tank from being empty throughout the year. The annual trend of SoC (Fig. 9) shows March as the critical month.

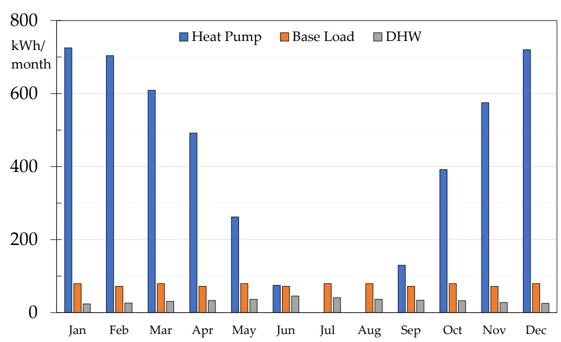

Fig. 8 – Monthly electric energy absorbed by the three consumption sources in the off-grid building

Table 1 – Main monthly results with PV=14.4 kW_p and V=5 m³

	PVS (kWh)	%PV	%AFC	H_2 Bal. (m³/month)	$\%E_{th,saved}$
J	522	58.8%	41.2%	-198.50	84.8%
F	719	71.8%	28.2%	-118.65	83.1%
M	1,252	78.6%	21.4%	9.70	80.3%
A	1,802	82.9%	17.1%	169.26	78.7%
M	2,209	81.1%	18.9%	304.36	76.7%
J	2,451	81.9%	18.1%	169.15	70.9%
J	2,607	80.1%	19.9%	29.21	73.8%
A	2,368	77.4%	22.6%	43.75	76.6%
S	1,688	72.7%	27.3%	-124.84	78.2%
O	1,284	74.0%	26.0%	46.77	79.2%
N	728	66.5%	33.5%	-115.92	82.2%
D	483	59.3%	40.7%	-206.75	83.8%
Y	***18,114***	***76.6%***	***23.4%***	***7.54***	***79.3%***

Moreover, the summer overproduction led to SoC>95% three times determining the electrolyzer switch-off, however hydrogen production restarted when SoC went down to 70%. In these cases, DHW reaches 80°C. Noticeably, the hydrogen volume at the end of the simulation is almost equal to the content at the start, therefore this configuration allows for a neutral yearly cycle that avoids storage issues over a long period.

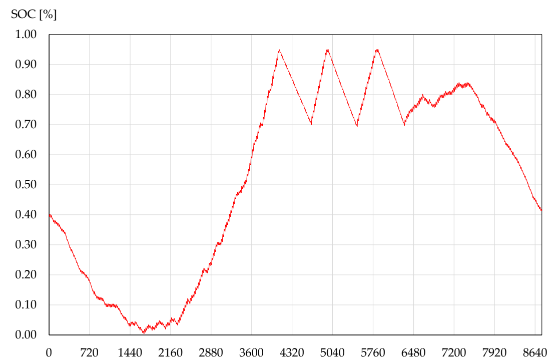

Fig. 9 – Yearly dynamic trend of the SoC regarding the hydrogen pressurized tank assuming PV=14.4 kW_p and V=5m³

If the plant configuration foresees a lower caption PV surface or a lower hydrogen tank volume, during winter there is no availability of hydrogen to supply the AFC. In these circumstances, Eq. 1 is not verified, but this could be overcome by avoiding the activation of the heat pump. This determines a worsening in terms of thermal comfort. Despite $\%E_{th,saved}$ being subjected to slight variation due to similar AFC operation time, indoor air temperatures often drop under 19 °C because the radiant floor is not supplied. Alternatively, the size of AFC can be reduced to absorb less hydrogen flow rates, but $\%E_{th,saved}$ reduces proportionally due to the lower recovered thermal energy, and again indoor air temperatures are negatively affected. This situation is depicted in Fig. 10 (3rd week of February) assuming PV=12.6 kW_P (14 panels in series arranged on two arrays), V=5 m³ and a smaller AFC made of 2 stacks in parallel with 24 cells in series that produces 1400 W (-25%). In contrast, if the PV size increases, also the hydrogen tank volume and the AFC size must be increased accordingly, due to the wider hydrogen availability. In particular, a greater PV peak power determines larger PV surpluses, therefore hydrogen production increases requiring larger gas tanks. Paradoxically, the recovered thermal energy recovered from the AFC decreases, because a large PV production produces a limitation of the AFC operative hours, and this aspect prevails on the thermal power growth achievable with the AFC size, as shown in Fig. 11, with evident deviances, especially in winter. Leaving the hydrogen storage at 5 m³, the available volume at the end of the year increases with the PV size, producing eventual issues in long-term tank management.

The effects related to the PV size on the accumulated hydrogen are depicted in Fig. 12. It can be appreciated that deviances are significant in winter, whereas the volumes tend to stabilize in summer for the intervention of the electrolyzer control (SoC > 0.95). It is confirmed that with the PV peak power growth, the hydrogen quantity to manage at the end of the year increases. Differences are significant in March: the hydrogen content in the tank increased by 36 Nm³, which becomes over 57 Nm³ passing to 21.6 kW_P. By setting the installed PV peak power and by varying the hydrogen storage volume (considering 6 and 7 m³) no evident deviances were detected and, consequently, not reported. The monthly percentage of the energy made available from the AFC as a function of the caption surface, setting V=5 m³, is shown in Fig. 13. As expected, the AFC contribution decreases with the PV peak power growth and in summer due to the large availability of solar irradiance. Therefore, to emphasize the micro-cogeneration features of the proposed system, the essential PV surface is recommended.

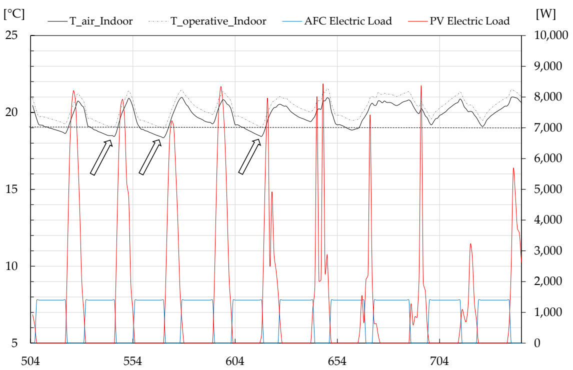

Fig. 10 – AFC production and indoor air temperature assuming PV=12.6 kW_P, V=5 m³ and a smaller AFC (undersized by 25%)

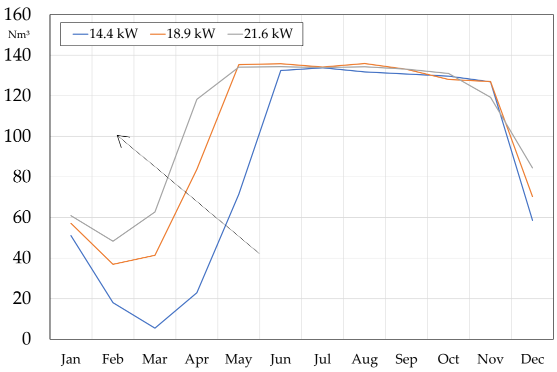

Fig. 12 – Trends of the stored hydrogen in the pressurized tank with V= 5 m³ varying the PV caption surface

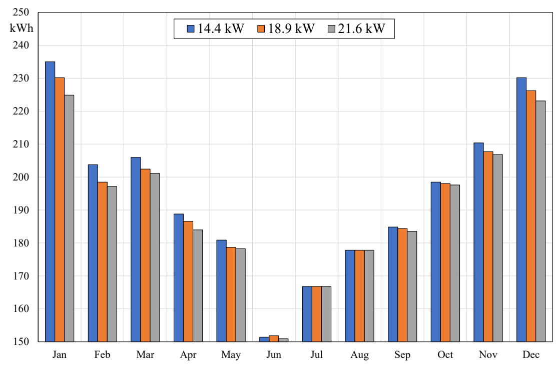

Fig. 11 – Recovered thermal energy with PV size, assuming V=5 m³ and AFC power of 1865 W

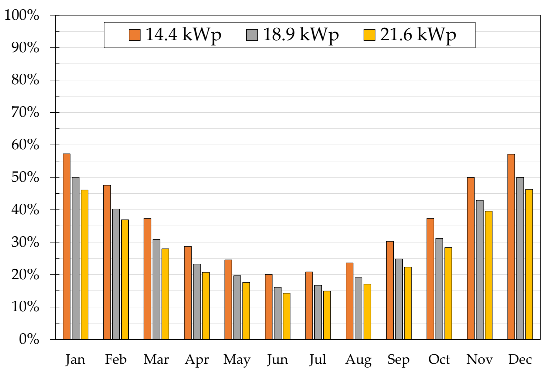

Fig. 13 – Percentage of the energy provided by the AFC with V= 5 m³ and varying the PV caption surface

3.1 Economic Evaluations

The studied system was compared with a plant configuration in which electric surpluses are managed by batteries. A capacity of 30 kWh, resulting from the average daily electric demand required in the critical month (January), was considered. The comparison was made in terms of Net Present Value (NPV) and Discounted Payback (DP). The considered costs are 1,500 €/kW$_P$ for PV panels and 600 €/kWh for batteries; regarding the hydrogen section: 10,125 € for AFC and auxiliaries, 15,000 € for electrolyzer and auxiliaries, 35,000 € for compressed hydrogen and oxygen storage in gas cylinders (Elassawi et al., 2023; Hassan et al., 2023). The AFC requires maintenance costs of 500 €/year, whereas the PV generator (periodic cleaning) of 360 €/year. The saved costs concern the avoided purchased electric energy, considering an item of 0,25 €/kWh, and the avoided gas consumption for DHW production (at 1.2 €/Sm^3) for the solution with batteries (being a not a cogeneration plant). Energy inflation and discount rates respectively of 8% and 4.5% were considered in a lifespan of 25 years. Precautionary, the AFC and electrolyzer replacement at the 15th year was assumed. The initial cost of € 81,725 is recovered in 14 years with an NPV of € 45,000, which becomes € 86,182 hypothesizing no replacements. The alternative solution costs € 36,000 with results listed in Tab. 2 considering different periods for the battery stock replacement. A longer PB than the proposed solution can be appreciated when batteries are replaced every 5 years. Similar NPVs are obtained if battery stock is replaced periodically every 6-7 years. The proposed system has an NPV better than the scenario with battery stock replaced every 10 years assuming an AFC duration of 15 years.

Table 2 – NPV and DP obtained for the alternative solution assuming different periods of the battery stock replacement

Battery replacement	NO replacement	After 5 years	After 10 years	After 15 years
NPV *(€)*	110,443	-41,112	50,632	80,938
DP *(year)*	8	>25	8	8

4. Discussion

TRNSYS simulations have allowed for identifying the main parameters affecting the design of a micro-cogeneration system conceived to ensure the energy self-sustainability of an isolated off-grid building based on a fuel cell supplied by hydrogen produced by electrolysis. Summarizing:

- AFC size must be calibrated considering the maximum absorption of the heat pump during winter nights when PV power is not available (the worst air-water heat pump operative conditions). Indeed, if AFC is undersized, discomfort risks occur because the heat pump cannot work due to the unavailability of the required electric power.
- PV peak power must be evaluated carefully because it determines the real share of electric surplus available for hydrogen production. If it is too low, the risk is to attain a building not energetically self-sustainable, but if it is too high the hydrogen overproduction makes its management difficult for a long period due to the achievement of saturated storage systems, both chemical and thermal.
- An increase in the PV size (to compensate for efficiency decrement due to panel ageing), must be combined with simultaneous gas-pressurized tank growth (modular system). But this reduces the AFC operation limiting the recovery of the thermal energy for producing DHW, and penalizing the performance of the micro-cogeneration system.
- Hydrogen acts as an inter-seasonal storage exploiting the summer overproduction.

5. Conclusion

For the reference building TRNSYS simulations have shown that:

- the optimized plant configuration requires 14.4 kW$_P$ of PV, a hydrogen gas tank of 5 m^3 and an AFC providing 1865 W at 220 V, satisfying simultaneously electric and thermal loads.
- An annual hydrogen balance of about 7 Nm^3 in the pressurized tank avoids the achievement of saturated storage systems in the long term.
- recovered heat allows a saving of almost 80% in the DHW demand;
- the considered micro-cogeneration system is profitable showing similar discounted payback to that achievable with electric storage made of

batteries replaced every 5 years, even assuming the AFC and electrolyzer change at the 15th year. A similar NPV is obtained assuming battery replacement every 6-7- years.

The reference building requires elevated electric loads in winter when PV production is low, confirming the system's goodness in difficult conditions. Results can be extended in localities with more favourable winter conditions by calibrating the sizes of PV and storage volume. In the future, analysis involving also summer cooling will be conducted.

References

Bevilacqua P., Morabito N., Bruno R., Ferraro V., Arcuri N. 2012. "Seasonal performances of photovoltaic cooling systems in different weather conditions". *Journ. of Clean* 275. https://doi.org /10.1016/j.jclepro.2020.122459

Dezhdar A., Assareh E., Agarwal N., Bedakhanian A., Keykhah S., Yeganeh Fard G., Zadsar N., Aghajari M., Lee M. 2023. "Transient optimization of a new solar-wind multi-generation system for hydrogen production, desalination, clean electricity, heating, cooling, and energy storage using TRNSYS". *Ren. Energy* 208: 512-537. https://doi.org/10.1016/j.renene.2023.03.019

Elassawy N.A., Rafea M.A., Roushdy N., Youssef M.E., Gouda M.H. 2023, "Development and evaluation of cost-effective and green Bi-functional nickel oxide decorated graphene electrocatalysts for alkaline fuel cells" *Results in Engineering* 17. https://doi.org /10.1016/j.rineng.2022.100871

Gugul G.N. 2023. "Optimum hybrid renewable energy system design for on and off-grid buildings: Hotel, education and animal hospital building case". *Solar Energy* 253: 414-427. https://doi.org /10.1016/j.solener.2022.12.044

Hakimi S.M., Hasankhani A. 2020. "Intelligent energy management in off-grid smart buildings with energy interaction". *Journal of Cleaner Production* 244. https://doi.org /10.1016/j.jclepro.2019.118906

Hassan Q., Sameen A.Z., Salman H.M., Jaszczur M., Al-Jiboory A.L. 2023, "Hydrogen energy future: Advancements in storage technologies and implications for sustainability", *Journal of Energy Storage* 72(B). https://doi.org /10.1016/j.est.2023.108404

Kallio S. and Siroux M. 2020. "Energy Analysis and Exergy Optimization of Photovoltaic-Thermal Collector". *Energies* 13(19). https://doi.org/10.3390/en13195106

Pflugradt N. 2024. "LoadProfileGenerator" https://www.loadprofilegenerator.de/

Perrella S., Bruno R., Bevilacqua P., Cirone D., Arcuri N. 2023. "Energy Evaluations of a New Plant Configuration for Solar-Assisted Heat Pumps in Cold Climates". *Sustainability* 15(2): 1663. https://doi.org/10.3390/su15021663

Saleem M.S., Abas N., Raza Kalair A., Rauf S., Haider A., Tahir M.S., Sagir M., 2020. "Design and optimization of hybrid solar-hydrogen generation system using TRNSYS". *International Journal of Hydrogen Energy* 45(32): 5814-15830. https://doi.org/10.1016/j.ijhydene.2019.05.188

UN Environmental Program. 2024. "Global Status Report for Buildings and Construction". https://wedocs.unep.org/bitstream/handle/20.500.11822/45095/global_status_report_buildings_construction_2023.pdf?sequence=3&isAllowed=y

VV.AA. 2018. "TRNSYS 18 Reference Manual", SEL, University of Wisconsin

Wei D, Zhang L., Alotaibi A.A., Fang J., Alshahri A.H., Almitani K.H. 2022. "Transient simulation and comparative assessment of a hydrogen production and storage system with solar and wind energy using TRNSYS International Journal of Hydrogen Energy 47(62): 26646-26653. https://doi.org /10.1016/j.ijhydene.2022.02.157

Zeng R., Tang X., Deng Y., Zhang X., Li H., Yin W., Zhang G. 2023. "Design and optimization of solar energy system with hydrogen energy storage and alkaline fuel cell". *Energy Conversion and Management* 295. https://doi.org /10.1016/j.enconman.2023.117628